Simulation of Wrinkle Formation in Free Electromagnetic Tube Compression

O. K. Demir, V. Psyk, A. E. Tekkaya

Institute of Forming Technology and Lightweight Construction, Technische Universität Dortmund, Dortmund, Germany

Abstract

A 3-dimensional (3D) finite element (FE) simulation of free electromagnetic (EM) tube compression was performed with the aim of predicting wrinkle formation. Staggered coupling was applied between the EM and mechanical parts of the problem. The full 360° portion of the problem was modelled since the wrinkle formation does not represent any symmetry in circumferential direction. The initial geometric imperfections of the tube were measured and included in the model to trigger buckling. The deformed geometry with the wrinkles could be predicted accurately.

Keywords

Electromagnetic tube compression, Buckling, Finite element simulation

1 Introduction

EM tube compression is the reduction of tube radius due to the application of radial electromagnetic forces. The material may buckle under the increasing circumferential compression during the inward motion, which causes wrinkles on the final product. This does not only prevent the acquirement of the desired shape, but also complicates the prediction of the formed geometry. However, a tool that can predict wrinkle formation could be used to optimize process parameters to minimize wrinkles, or to demonstrate ways to avoid them, e.g. mandrel usage, or to reverse them, e.g subsequent hydroforming or EM expansion.

In a homogenously compressed body geometric or material imperfections trigger buckling. Because of that, researchers tried to predict wrinkles by simulations including the initial imperfections of the workpiece (WP). However, inadequacy of the simulation tools or harsh assumptions avoided good correspondence with the experimental results. The aim of the present study is to calculate wrinkles in free EM tube compression by a coupled 3D FE simulation.

2 State of the Art

In EM forming (EMF), a highly damped alternating current is sent through a coil in tens of microseconds. This current creates a counter current in the WP. The repulsive forces between the two currents form the WP. A tube is placed inside a solenoid for the EM compression.

Kirkpatrick and Holmes (1988) calculated wrinkling of tubes under radial explosive loading by means of FE method and shell elements. They showed the importance of including the correct initial geometrical imperfections in wrinkle prediction.

Min and Kim (1993) measured the magnetic flux during EM tube compression experiments and calculated the magnetic pressure vs. time from the flux. They applied this pressure uniformly on the outer wall and simulated the deformation with a 3D dynamic explicit FE method. The tube was modelled with solid elements, one in thickness direction. The initial imperfections were represented by an initial displacement perturbation given by

$$W(\theta) = \sum_{n=1}^{n_c} a_n \cos(n\theta + \phi_n), \tag{1}$$

where θ is the hoop angle, n is the mode number, a_n is the amplitude of the displacement perturbation, and ϕ_n is the phase angle. a_n was calculated with regard to roundness measurements, and random values were used for ϕ_n. The contribution of modes larger than a certain critical value of n_c was disregarded. 35 mm long Ø40 mm tubes were formed with coils longer then the tubes. The tubes were crushed and the resulting shapes were very complex to simulate accurately. The correspondence with the experimental results was better when a mandrel was used, especially at high energy values, when the tube was more ironed on the mandrel.

3 The Proposed Method

In order to predict the wrinkles due to EM compression accurately the initial imperfections must be included directly in the FE model and a simulation must be performed, in which the mechanical and the EM parts of the problem are coupled. The success of this method was demonstrated by comparing the simulation results with the experiment results in case of free compression of an aluminum tube.

4 Experimental Setup and Measurements

A 110 mm long, 2 mm thick Ø40 mm EN-AW 6060 tube in T6 condition was compressed. A 55 mm long copper coil with an inner diameter of 41.7 mm was used. The coil cross-section was rectangular with the dimensions: 13.7 mm width – 5.0 mm height. The resistivities of the tube and coil materials were measured as 2.94×10^{-8} Ωm and 1.79×10^{-8} Ωm, respectively.The compression was performed with a sudden release of 5 kJ energy stored in four capacitors with a total capacitance of 992 μF. The used machine had an inner inductance of 50 nH and an inner resistance of 3.3 mΩ.

Total current flowing through the coil during deformation was measured using a Rogowski coil, and is given in Figure 1a. The inner and outer contours of the unformed tube were measured using a 3D coordinate measuring device. The measurements were done at a single point along the axis. That is, the cross-sectional geometry was assumed to be uniform in axial direction. This was done depending upon the fact that the tubes were manufactured by profile extrusion. The measured initial contours are given in Figure 1c. According to those, the tube thickness changes between 1.95 mm and 2.07 mm. Data in Figure 1a and Figure 1c were then introduced as input to the simulations. The formed shapes were measured with a 3D digitizer to compare with the simulation results.

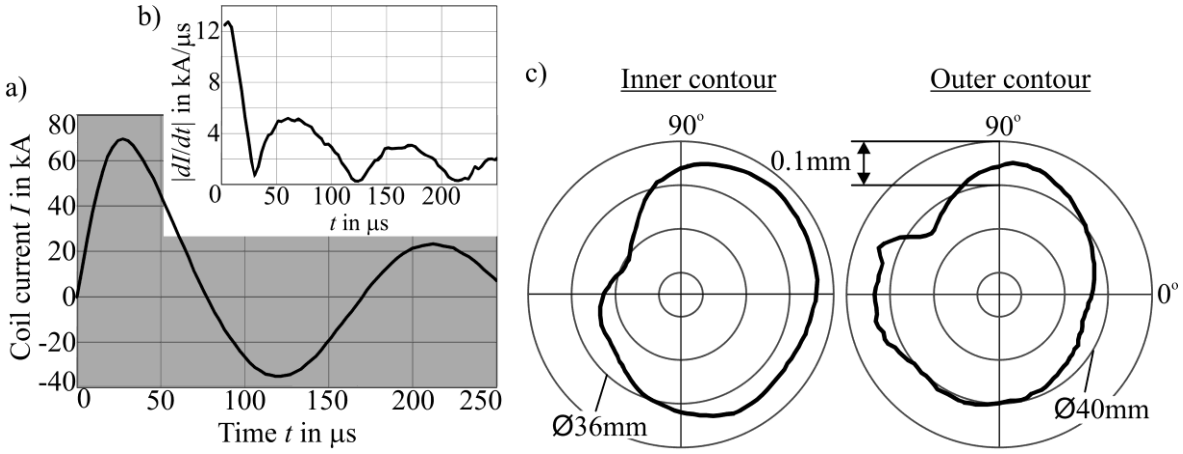

***Figure 1**: a) Measured coil current b) Slope of coil current c) Initial tube geometry*

5 Simulation of EMF

Before simulating the compression under EM forces, these forces must be calculated with a transient EM calculation. The thermal side of the problem was not taken into consideration in order to reduce the calculation time. That is, plastic heating and heating due to electrical resistance, and their effects on electrical resistivity and mechanical properties were neglected. In what follows, the principles of the EM and mechanical solutions, and the coupling between them are explained.

5.1 EM Problem

The EM problem consists of the four Maxwell Equations:

$$\vec{\nabla} \times \vec{B} = \mu_0 \left(\vec{J}_{tot} + \varepsilon_0 \frac{\partial \vec{E}}{\partial t} \right), \tag{2}$$

$$\vec{\nabla} \times \vec{E}_{ind} = -\frac{\partial \vec{B}}{\partial t}, \tag{3}$$

$$\vec{\nabla} \circ \varepsilon_0 \vec{E} = \rho_{tot}, \tag{4}$$

$$\vec{\nabla} \circ \vec{B} = 0. \tag{5}$$

Here, $\vec{B}$ is the magnetic field, $\vec{E}$ is the electric field, $\vec{J}_{tot}$ is the total current density, $\vec{E}_{ind}$ is the induced electric field, and ρ_{tot} is the total charge density. μ and ε are the magnetic permeability and electric permittivity, respectively. μ_0 and ε_0 are those of vacuum. $\circ$, $\times$, and $\vec{\nabla}$ denote dot-product, cross-product, and del operator, respectively.

According to Eq. 2 an electric current ($\vec{J}_{tot}$) and/or a changing electric field ($\partial\vec{E}/\partial t \neq 0$) produce a circulating magnetic field. In case of EMF the frequency of the excitation current (coil current) is too low to take the latter into account (low frequency assumption). This reduces Eq. 2 to:

$$\vec{\nabla} \times \vec{B} = \mu_0 \vec{J}_{tot} . \tag{6}$$

$\vec{J}_{tot}$ is the sum of conduction ($\vec{J}_{con}$), polarization ($\vec{J}_{pol}$), and magnetization ($\vec{J}_{mag}$) currents. Low frequency assumption neglects polarization ($\vec{J}_{pol} = \vec{0}$). $\vec{J}_{mag}$ emerges from the magnetization of the media under the application of a magnetic field. A media is magnetized to the extent of its permeability μ. If μ is used instead of μ_0 in Eq. 6, $\vec{J}_{tot}$ does not have to include $\vec{J}_{mag}$, since the magnetization effect is regarded by the parameter μ. Accordingly, Eq. 2 takes the form:

$$\vec{\nabla} \times \vec{B} = \mu \vec{J}_{con} . \tag{7}$$

The coil current in EMF is an alternating conductive current. By virtue of Eq. 7 it creates an alternating magnetic field. Eq. 3 reveals that an alteration in the magnetic field induces a circulating electric field ($\vec{E}_{ind}$). If a conducting material is present $\vec{E}_{ind}$ drives a circulating electric current according to:

$$\vec{J}_{con} = \frac{\vec{E}}{\rho} , \tag{8}$$

where ρ denotes the resistivity of the material. In EMF the conducting material is the WP, and the circulating currents are the so called eddy currents. Any charge moving in a magnetic field experiences Lorentz forces given by Eq. 9. Lorentz forces on the eddy currents are the triggering forces of EMF.

$$\vec{F} = \vec{J} \times \vec{B} . \tag{9}$$

Knowing the coil current for a certain time interval, the Maxwell equations can be solved for a given spatial configuration of the objects. The result is the $\vec{B}$ and $\vec{E}$ distributions with respect to time. Equations 8 and 9 give, then, the force distribution on the WP. This was accomplished by the commercial implicit FE code ANSYS/EMAG.

5.1.1 FE Model for EM Calculation

A quarter portion of the model is displayed in Figure 2, although the whole 360° was simulated. A ½ model was utilized owing to the mirror symmetry. The circumferential dimensions of the elements were 3° except in the core region. A time-step of 1 μs was used for the calculation after a sensitivity study of the total force on the WP.

The *skin effect* was taken into account while determining the mesh for the cross-section (z=0 surface) shown in Figure 2. The eddy currents whirl in such a manner that they oppose the *change* in the magnetic field created by the coil current. In other words, they resist the penetration of the magnetic field into the WP. The strength of this resistance is directly proportional to the *change* in the coil current, i.e., the slope of the current. Due to damping this slope decreases during the process (see Figure 1b). As a result, on one hand, at the beginning of the process no magnetic field can be seen except at the *skin* of the WP. On the other hand, towards the end of the process the magnetic field penetrates the WP, and even passes through it, reaching the inside of the tube. In order to calculate the magnetic field at the beginning of the process accurately, a finer mesh must be used at the outer regions of the tube's wall thickness. However, a very coarse mesh cannot be used at the inner regions and inside of the tube because of the penetration taking place towards the end of the process.

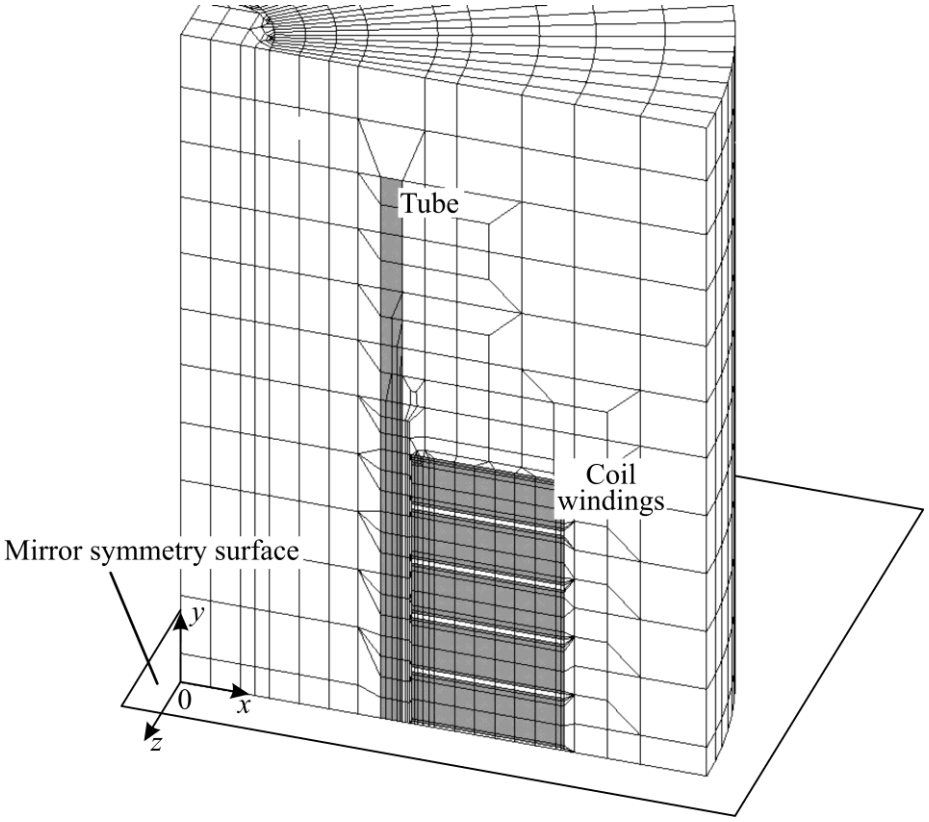

***Figure 2**: Quarter of the initial FE model for EM calculation*

This situation is valid also for the coils. The total current flowing through a winding is given as input (Figure 1a). However, the distribution must be determined by the FE calculation. Due to the skin effect the current tends to flow at the outer regions. Hence, a finer mesh is needed at the outer regions.

5.2 Mechanical Problem

After the EM solution for a certain time interval, the obtained nodal forces can be used for the forming simulation. This was accomplished by the commercial dynamic explicit FE code LS-DYNA. The tube mesh (3D continuum elements with 8 nodes) from the EM calculation was transferred to a mechanical model. Reduced integration scheme was employed. The strain rate dependent flow curve for the tube material was taken from [3].

5.3 Coupling

The EM forces on the WP are dependent on its spatial configuration, which is changing throughout the process due to deformation. Hence, the spatial configuration used for the EM simulation must be updated continuously during the calculation. This update is called the coupling of the EM and mechanical parts of the simulation. Such a simulation of EMF is called a coupled simulation. In the following the factors necessitating the coupling and the strategies to accomplish it are examined.

The effect of change of spatial configuration can be neglected in two cases. First, if the coil current that is creating the forces damps out before a significant WP move. This assumption was used in many early modelling efforts of EM sheet metal forming as stated by El-Azab et al. (2003) in their review paper on modelling of EMF. Second, if the calculation is going to be used only for small strains, for instance, in case of calibration processes. Iriondo (2007) simulated calibration processes uncoupled, owing to this assumption. Simulation of tube compression cannot be classified into both groups and demands a coupled calculation. Kleiner and Brosius (2006) showed that the correspondence with the experimental results show a significant improvement in case of coupling.

There are two coupling strategies. In monolithic coupling one set of equations is solved with degree of freedoms from both mechanical and EM problems. Excluding the work of Karch and Roll (2005) monolithic coupling could not find any application in EMF simulation yet, because of its difficulty and expense. In staggered (loose, weak) coupling EM and mechanical analyses are performed sequentially in a loop. This method has been applied by several researchers following Bendjima (1997) and Fenton and Daehn (1998). ANSYS/EMAG and LS-DYNA were coupled by Oliveira (2002) for 3D sheet metal forming.

In the present study, staggered coupling was utilized. In staggered coupling the EM simulation is interrupted regularly in order to update the WP geometry. A major difficulty emerges due to this interruption. The media between the conducting objects (air) must also be meshed in an EM FE simulation. When the WP geometry is updated the air geometry must also be modified accordingly. Oliveira (2002) accomplished this by including the air also in the structural simulation. He stated that the material properties selected for the air are very important for the air elements to keep acceptable aspect ratios throughout the simulation. In the present work the air mesh was morphed corresponding to the calculated tube deformation before every EM simulation.

A sensitivity study performed by Demir et al. (2009) showed that the converged result can be obtained when the interval for geometry update is selected as 2 μs.

6 Results and Discussion

Comparison of calculated and measured tube geometries are given in Figure 3.

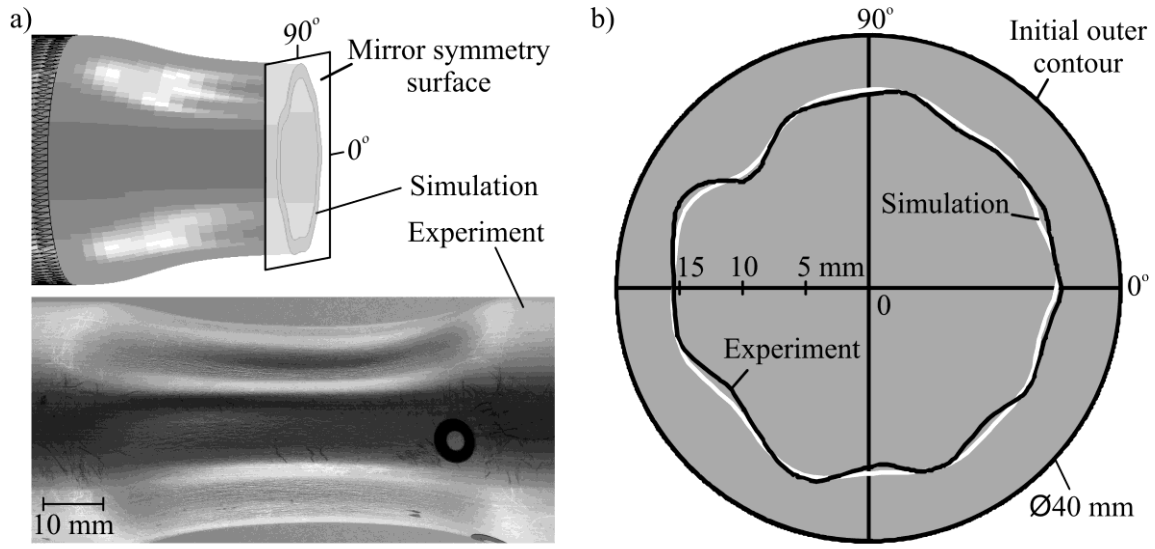

***Figure 3**: a) Simulated and measured tube geometries. b) Simulated and measured outer contours at the mirror symmetry surface*

Psyk et al. (2005) reported that the deteriorations of the initial tube roundness are intensified by the compression process. A comparison between Figure 3b and Figure 1b confirms this result. The compressed shape reflects the initial roundness. For instance, the gross wrinkle at approximately 135° is caused by the gross deterioration of the outer roundness at that region.

Figure 3a shows that the wrinkles' forms do not change in axial direction. Their intensity changes merely. So it is a justified assumption that the initial imperfections of the cross-section geometry are uniform along the axis. It is also reasonable to use mirror symmetry in the simulation.

The possible reasons for the slight discrepancy between the simulation and experimental results seen in Figure 3b are insufficient element partition in circumferential direction and thermal effects. The circumference was divided into 120 equal parts. A sensitivity study with respect to that parameter is yet to be performed. Kirkpatrick and Holmes (1988) showed that the geometry of the wrinkles can be better predicted when the number of elements per wrinkle increases. Thermal effects were neglected. Karch and Roll (2005) detected an approximately 90° increase in WP temperature (Ø40 mm EN-AW 6060 tubes) during EM compression by means of 2D axisymmetric simulations. This should change the electrical and mechanical properties of the WP. More accurate results can be obtained when the combined effect of temperature increase and high strain rate is taken into consideration.

7 Conclusion

The wrinkle formation in free EM tube compression can be simulated by a 3D staggered coupled EMF simulation. The initial geometrical imperfections must be included in the model in order to predict the final geometry accurately. The correspondence between the experimental and simulation results is acceptable, although the thermal effects were not taken into consideration. Other cases with varying geometries, materials, and process parameters must also be simulated to free the conclusion from being specific.

The simulation tool can be used for process design for a given exact initial geometry. However, it is not practical to measure the actual initial imperfections for every WP. This problem can be solved in two ways. First, seamless tubes coming from the same source (a combination of dies and process parameters) will have the same cross-section because of the steady-state nature of the profile extrusion process. A single measurement for a group of tubes will be adequate. Second, instead of the exact initial geometry, random imperfections, which are created according to the known geometry tolerances, can be taken into account. The simulation tool can also be used to decide on the allowable initial geometry tolerances to manufacture a given product.

Acknowledgements

This work is based on the results of the research group PAK343; the authors would like to thank the German Research Foundation for its financial support.

The EMF machine is a 7000 Series MAGNEFORM, manufactured by MAXWELL and modified by POYNTING. The 3D coordinate measuring device is from the company ZEISS. 3D digitizing was performed using the ATOS system from the company GOM.

References

[1] *Kirkpatrick, S. W.; Holmes, B. S.*: Structural response of thin cylindrical shells subjected to impulsive external loads. AIAA Journal, 26, p. 96-103, 1988

[2] *Min, D. K.; Kim, D. W.:* A finite-element analysis of the electromagnetic tube-compression process. Journal of Materials Processing Technology, 38, p. 29-40, 1993

[3] *Demir, O. K.; Psyk, V.; Tekkaya, A. E.*: Simulation of tube wrinkling in electromagnetic compression. Proceedings of ICAFT 2009, Chemnitz, Germany, p. 121-135, 2009

[4] *El-Azab, A.; Garnich, M.; Kapoor, A.*: Modeling of the electromagnetic forming of sheet metals: State-of-the-art and future needs. Journal of Materials Processing Technology, 142, p. 744-754, 2003

[5] *Iriondo, E.*: Electromagnetically Impulsed Springback Calibration. Ph.-D.-Dissertation, The University of the Basque Country, 2007

[6] *Kleiner, M.; Brosius, A.*: Determination of flow curves at high strain rates using the electromagnetic forming process and an iterative finite element simulation scheme. Annals of the CIRP, 55/1, 2006

[7] *Karch, C.; Roll, K.*: Transient simulation of electromagnetic forming of aluminium tubes. Advanced Materials Research, 6-8, p. 639-646, 2005

[8] *Bendjima, B.*: Finite element modelling of electromagnetic phenomena related to electromagnetic forming. Doctoral Thesis, University of Nantes, France, 1997

[9] *Fenton, G. K.; Daehn, G. S.*: Modeling of electromagnetically formed sheet metal. Journal of Materials Processing Technology, 75, p. 6-16, 1998

[10] *D. A., Oliveira*: Electromagnetic forming of aluminum alloy sheet: experiment and model. Masters thesis, University of Waterloo, Canada, 2002

[11] *Psyk, V.; Beerwald, C.; Homberg, W.; Kleiner, M.*: Extension of Forming Limits by Using a Process Combination of Electromagnetic Forming and Hydroforming. Proceedings of the 8th Int. Conf. on Technology of Plasticity (ICTP) 2005, Verona, Italy, 2005